Self-Assembled Mesoporous Silica−Germania Films

Stefano Costacurta,[†] Luca Malfatti,[†] Tongjit Kidchob,[†] Masahide Takahashi,[†,‡] Giovanni Mattei,[§] Valentina Bello,[§] Chiara Maurizio,[⊥] and Plinio Innocenzi*[,†]

Laboratorio di Scienza dei Materiali e Nanotecnologie, D.A.P., Università di Sassari, Nanoworld Institute and INSTM, Palazzo Pou Salit, Piazza Duomo 6, 07041 Alghero (SS), Italy, Institute for Chemical Research, Kyoto University, Uji, Kyoto 611-0011, Japan, Dipartimento di Fisica "Galileo Galilei", Università di Padova, Via Marzolo 8, 35131 Padova, Italy, and CNR-INFM c/o European Synchrotron Radiation Facility, 6 rue J. Horowitz, 38043 Grenoble, France

Received September 17, 2007. Revised Manuscript Received February 13, 2008

Silica−germania thin films are important materials for photonic applications, but synthesis of these films is quite difficult to achieve especially with the task of obtaining a homogeneous structure. We have prepared mesoporous silica−germania films via evaporation-induced self-assembly from ethanolic solutions of Si and Ge chlorides, using a triblock copolymer as the templating agent. The mesostructure has been found to have tetragonal symmetry, and the degree of order decreased with increasing Ge content. X-ray photoelectron spectroscopy has shown that the chemical composition of the films is close to the nominal composition. Infrared analysis has revealed that the pore walls are highly condensed and residual hydroxyls are present as isolated or hydrogen bonded silanols in short chains. UV−vis absorption and photoluminescence spectra have been correlated with the presence of photoactive oxygen-deficient Ge^{2+} centers which can give rise to a variation in the refractive index upon high-power density UV irradiation.

Introduction

Mesoporous ordered films are a promising category of functional materials for applications in high-technology, such as photonics,[1] sensing,[2] and electronics, due to high specific surface area, pore size that can be tailored in the nanometer range, and possibility to incorporate functional groups or immobilizing active molecules in the mesopores or in the inorganic network.[3,4] Mesoporous films are typically synthesized by evaporation-induced self-assembly (EISA) via dip- or spin-coating, using inorganic precursors such as alkoxides, organo-alkoxides, or chlorides and organic templating agents such as low-molecular weight surfactants or amphiphilic block copolymers. Much of the research in this field has been devoted to silica and titania mesoporous films because of the broad range of applications and because they serve as models to understand the physicochemical phenomena occurring during self-assembly.[5–7] Other compositions of mesoporous films have been explored, most notably transition metal oxides, organic−inorganic hybrids,[8] and phosphates.[9]

Silica−germania glasses are of particular importance, especially for applications in photonics, such as fibers and optical waveguides;[10] for example, fiber Bragg gratings are based on photoactivated processes[11,12] and a large second order nonlinearity can be induced by UV-light assisted poling.[13] Silica−germania films exhibit photoactive properties,[14,15] and the divalent Ge^{2+} centers can be photobleached and oxidized to tetravalent Ge^{4+} centers, causing a local densification of the inorganic network, thus increasing the refractive index (typically on the order of 10^{-4}−10^{-5}). The low phononic energy of germania-based glasses can be used to obtain low-loss optical waveguides and amplifiers in thin silica−germania films.[16] Sol−gel processing represents an important method to fabricate silica−germania films and

* Corresponding author. E-mail: plinio@uniss.it.
[†] Università di Sassari.
[‡] Kyoto University.
[§] Università di Padova.
[⊥] CNR-INFM c/o European Synchrotron Radiation Facility.

(1) (a) Wirnsberger, G.; Yang, P.; Huang, H. C.; Scott, B.; Deng, T.; Whitesides, G. M.; Chmelka, B. F.; Stucky, G. D. *J. Phys. Chem. B* **2001**, *105*, 6307. (b) Yang, P.; Wirnsberger, G.; Huang, H. C.; Cordero, S. R.; McGehee, M. D.; Scott, B.; Deng, T.; Whitesides, G. M.; Chmelka, B. F.; Buratto, S. K.; Stucky, G. D. *Science* **2000**, *287*, 465.
(2) (a) Innocenzi, P.; Martucci, A.; Guglielmi, M.; Bearzotti, A.; Traversa, E.; Pivin, J. C. *J. Eur. Ceram. Soc.* **2001**, *21*, 1985. (b) Innocenzi, P.; Martucci, A.; Guglielmi, M.; Bearzotti, A.; Traversa, E. *Sens. Actuators, B* **2001**, *76*, 299. (c) Bearzotti, A.; Bertolo, J. M.; Innocenzi, P.; Falcaro, P.; Traversa, E. *J. Eur. Ceram. Soc.* **2004**, *24*, 1969.
(3) Soler-Illia, G.; Sanchez, C.; Lebeau, B.; Patarin, J. *Chem. Rev.* **2002**, *102*, 4093.
(4) Angelomé, P. C.; Fuertes, M. C.; Soler-Illia, G. *Adv. Mater.* **2006**, *18*, 2397.
(5) Tate, M. P.; Urade, C. N.; Kowalski, J. D.; Wei, T.-C.; Hamilton, B. D.; Eggiman, B. W.; Hillhouse, H. W. *J. Phys Chem. B* **2006**, *110*, 9882.
(6) Innocenzi, P.; Malfatti, L.; Kidchob, T.; Costacurta, S.; Falcaro, P.; Piccinini, M.; Marcelli, A.; Morini, P.; Sali, D.; Amenitsch, H. *J. Phys. Chem. C* **2007**, *111*, 5345.
(7) Crepaldi, E. L.; Soler-Illia, G.; Grosso, D.; Cagnol, F.; Ribot, F.; Sanchez, C. *J. Am. Chem. Soc.* **2003**, *125*, 9770.
(8) Soler-Illia, G.; Innocenzi, P. *Chem.—Eur. J.* **2006**, *12*, 4478.
(9) Nishiyama, Y.; Tanaka, S.; Hillhouse, H. W.; Nishiyama, N.; Egashira, Y.; Ueyama, K. *Langmuir* **2006**, *22*, 9469.
(10) Hirai, Y.; Fukuda, T.; Kubota, K. *J. Non-Cryst. Solids* **1987**, *93*, 431.
(11) Hill, K. O.; Fuji, Y.; Johnson, D. C.; Kawasaki, B. S. *Appl. Phys. Lett.* **1978**, *32*, 647.
(12) Othonos, A.; Kalli, K. *Fiber Bragg Gratings: Fundamentals and Applications in Telecommunications and Sensing*; Artech House: Norwood, MA, 1999; Chapter 2.
(13) Fujiwara, T.; Takahashi, M.; Ikushima, A. J. *Appl. Phys. Lett.* **1997**, *71*, 1032.
(14) (a) Hosono, H.; Abe, Y.; Kinser, D. L.; Weeks, R. A.; Murata, K.; Kawazoe, H. *Phys. Rev. B* **1992**, *46*, 11445. (b) Hosono, H.; Kawazoe, H.; Muta, K. *Appl. Phys. Lett.* **1994**, *64*, 282.
(15) Nishii, J.; Fukumi, K.; Yamanaka, H.; Kawamura, K.; Hosono, H.; Kawazoe, H. *Phys. Rev. B* **1995**, *52*, 1661.
(16) (a) Martucci, A.; Brusatin, G.; Guglielmi, M.; Strohhofer, C.; Fick, J.; Pelli, S.; Righini, G. C. *J. Sol-Gel Sci. Technol.* **1998**, *13*, 535. (b) Strohhofer, C.; Capecchi, S.; Fick, J.; Martucci, A.; Brusatin, G.; Guglielmi, M. *Thin Solid Films* **1998**, *326*, 99.

10.1021/cm8000249 CCC: $40.75
Published on Web 04/23/2008

several examples have been reported.[17–19] The synthesis is not simple; the high reactivity of germanium precursors, in fact, needs to be adjusted to that of silicon alkoxides to avoid phase separation.[20] The homogeneity of the material and the amount of hydroxyl species has to be carefully evaluated in the case of photonic applications. SiO_2-GeO_2 sol−gel films can be produced as pure oxides or hybrid organic−inorganic films,[17c,21] but the film processing has to face several severe problems in order to be used in photonics. A high temperature is necessary to condensate the oxide structure and to reduce the hydroxyl content. At around 600 °C, however, germania crystallizes and this results in a decrease of oxygen vacancies.[29] Alternatively, a thermal treatment (∼500 °C) in H_2 reducing atmosphere can be performed in order to increase the amount of defects.[14] Even if crystallization does not occur below 500 °C, Ge-OH species can be produced via diffusion of hydrogen atoms. Another problem is that the thermal treatment in sol−gel films induces a stress that at 500 °C is not completely released.[22] In hybrid organic−inorganic materials, even low temperatures (between 100 and 300 °C) significantly decrease the concentration of defects. The possibility of producing SiO_2-GeO_2 films at low processing temperatures, with a small residual stress and with a high content of Ge^{2+} centers without using a specific reducing treatment, represents, therefore, a challenging opportunity to explore. An interesting question is how the presence of a porous structure can affect the optical properties of a silica−germania material. The interest arises because the combination of photoactivity with the mesoporous structure could allow the fabrication of sensing and photonic devices with integrated functions that can, at least in part, overcome the problems related to sol−gel films processing. In fact, due to the high porosity, the inorganic lattice can increase the density to a higher extent upon UV irradiation.[23] Furthermore, the amount of Ge^{2+} centers is expected to be larger than in nonporous silica−germania films obtained by sol−gel due to the high specific surface area of mesoporous films: most of silica and germania units are located at the solid−air interface and in this region the bonds are strained. On the other hand by changing the processing parameters of the mesoporous films, such as overall porosity, pore dimension and shape, and pore organization, we can expect to tune the optical properties. This is much more difficult to achieve in dense films; therefore, the presence of mesoporosity is expected to affect the final property of the material and the photoactive response of silica−germania films.

In the present work we report the synthesis of mixed SiO_2-GeO_2 mesoporous films showing the presence of photoactive Ge-related defects, which is a prospects in the application as photosensitive materials. Such materials can also be suitable in the viewpoint of fundamental science, in that these films are good candidates to investigate surface defects.[24]

Experimental Section

Four precursor solutions were prepared, adding different amounts of anhydrous $SiCl_4$ and $GeCl_4$ under stirring to a stock solution of Pluronic F127 dissolved in ethanol. The molar ratios were set to $EtOH/GeCl_4/SiCl_4/F127 = 30:x:(1-x):0.005$, where x was varied between 0.1 and 0.4 (samples with different compositions are referred to as SG1, SG2, SG3, and SG4, indicating [Ge]/[Si] = 0.1, 0.2, 0.3, 0.4, respectively). The substrates were dip-coated on the fresh solution at the pulling rate of 2 $mm \cdot s^{-1}$; the relative humidity (RH) in the deposition chamber was set to 24 ± 2%. The substrates were either silicon wafers (100-oriented, B-doped test grade, nominal thickness 500 μm) or fused silica slides (UV grade, thickness 1 mm). The solutions were turbid, and a white precipitate was observed if stirring was stopped, probably due to aggregation between surfactant molecules. Therefore, solutions were sonicated for 5 min prior to each dip-coating in order to redissolve the precipitate and ensure homogeneity of films. Two minutes after dip-coating the films were transferred into a furnace at the temperature of 100 °C, and then they were calcined at 350 °C or higher temperatures for 1 h; the thermal treatments were all performed in air.

Grazing incidence small-angle X-ray scattering (GISAXS) measurements were performed at the European Synchrotron Radiation Facility (ESRF) in Grenoble, France, at the ID01 beamline. The incident energy of 8 keV ($\lambda = 1.54$ nm) was selected, and the glancing angle was adjusted slightly above the critical angle (∼0.2°). The diffraction patterns were collected with a two-dimensional CCD detector. A silver behenate powder standard ($d = 58.38$ Å) in a capillary glass was used for calibration. Data analysis was carried out using software Fit2d.[25]

Transmission electron microscopy (TEM) characterization was performed with a field-emission gun FEI TECNAI F20 SuperTwin FEG-(S)TEM microscope operating at 200 kV equipped with an EDAX energy dispersive X-ray spectrometer (EDS). The samples were prepared as cross-sections cutting the mesoporous films along two perpendicular directions with respect to the Si substrate. The ordered sample phase was investigated by acquiring TEM images in scanning mode (STEM) in which a small electron probe (about 1 nm fwhm) is rastered over the sample.

The chemical analysis of the mesoporous silica−germania films was carried out by using an ULVAC-PHI 5500 X-ray photoelectron spectrometer with Mg Kα radiation operated at 15 kV and 20 mA.

Fourier transform infrared spectroscopy (FTIR) was performed with a Nicolet Nexus FTIR spectrophotometer equipped with a KBr-DTGS detector and a KBr beamsplitter, in the 4000−400 cm^{-1} range. The spectra were recorded in transmission mode on films deposited on Si wafers, and the background was recorded using a Si substrate. Each acquisition was the average of 256 scans collected with a resolution of 4 cm^{-1}. Data analysis was performed on Bruker Opus 5.5 software: in particular, the baseline was calculated by concave rubberband correction using 64 points and 5 iterations.

(17) (a) Brusatin, G.; Guglielmi, M.; Martucci, A. *J. Am. Ceram. Soc.* **1997**, *80*, 3139. (b) Grandi, S.; Mustarelli, P.; Agnello, S.; Cannas, M.; Canonizzo, A. *J. Sol-Gel Sci. Technol.* **2003**, *26*, 915. (c) Que, W. X.; Hu, X.; Zhang, Q. Y. *Appl. Phys. B: Laser Opt.* **2003**, *76*, 423.
(18) (a) Ho, C. K. F.; Djie, H. S.; Pita, K.; Ngo, N. Q.; Kam, C. H. *Electrochem. Solid-State Lett.* **2004**, *7*, 96. (b) Simmons, K. D.; Potter, B. G.; Stegeman, G. I. *Appl. Phys. Lett.* **1994**, *64*, 2537. (c) Simmons, K. D.; Stegeman, G. I.; Potter, B. G.; Simmons, J. H. *Opt. Lett.* **1993**, *18*, 25.
(19) Rajni, Ho.; Pita, K.; Tjin, S. C.; Yu, S. F.; Kam, C. H. *Appl. Phys. A: Mater. Sci. Process.* **2006**, *82*, 535.
(20) Alonso, B.; Dominique, D.; Babonneau, F.; Brusatin, G.; Della Giustina, G.; Kidchob, T.; Innocenzi, P. *Chem. Mater.* **2005**, *17*, 3172.
(21) Que, W.; Hu, X. *Opt. Mater.* **2004**, *27*, 273.
(22) Kozuka, H. *J. Sol-Gel Sci. Technol.* **2006**, *40*, 287.
(23) Sakoh, A.; Takahashi, M.; Yoko, T.; Nishii, J.; Nishiyama, H.; Miyamoto, I. *Opt. Express* **2003**, *11*, 2679.
(24) Skuja, L. *J. Non-Cryst. Solids* **1998**, *239*, 16.
(25) http://www.esrf.eu/computing/scientific/FIT2D/ (accessed June 2007).

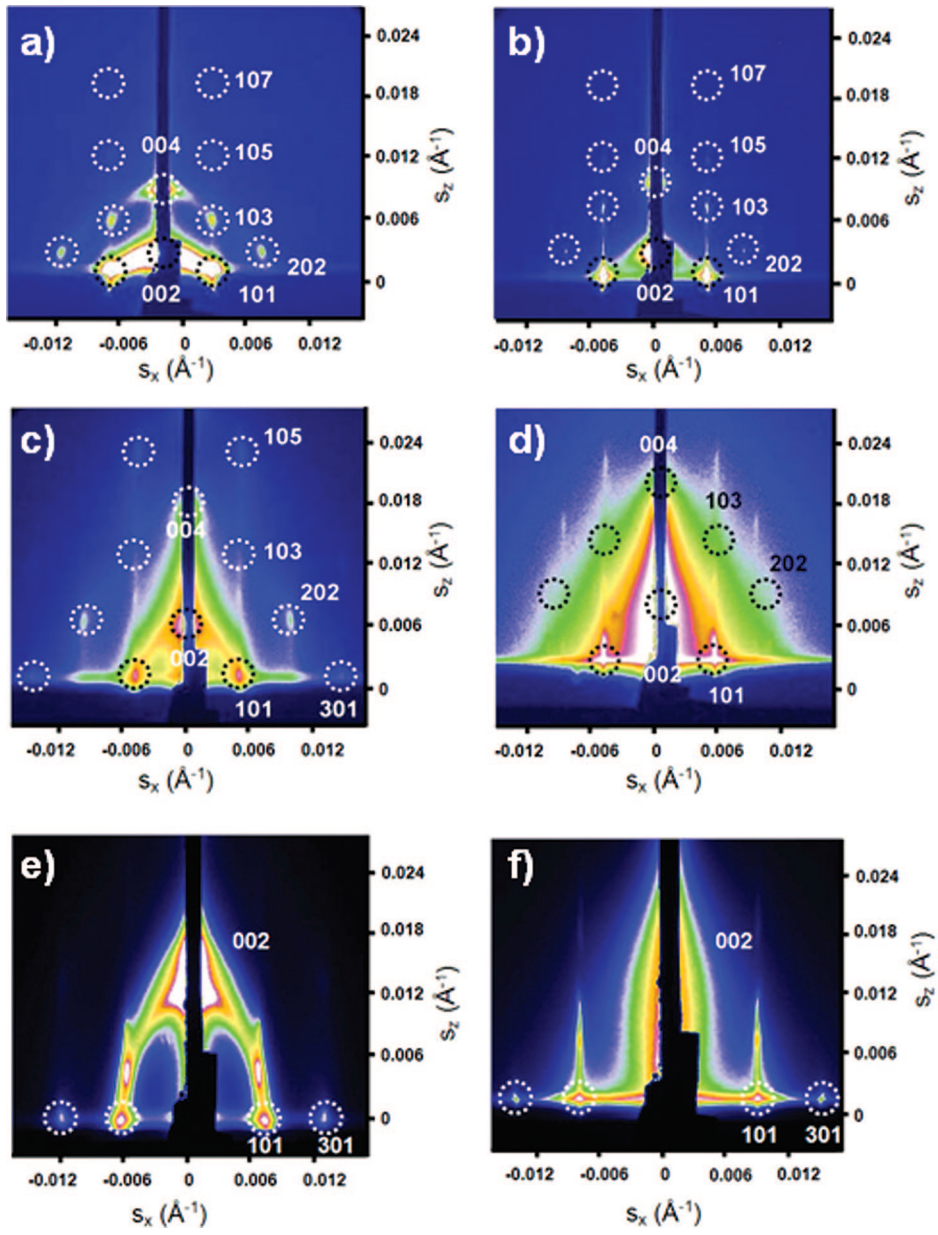

Figure 1. GISAXS patterns referring to sample SG1 ([Ge]/[Si] = 0.1), thermally treated at 100 (a), 350 (c) and 550 °C (e). Sample SG2 ([Ge]/[Si] = 0.2), thermally treated at 100 (b), 350 (d) and 550 °C (f).

Film thickness was measured by spectroscopy ellipsometry working in the 390−900 nm range. (αSE, J.A.Woollam, U.S.A.). A Bruggeman effective medium approximation (EMA) layer with two components (Cauchy film and void) was used to evaluate the optical constants. The quality of the fitting was evaluated on the ground of the mean square error (MSE).

The optical absorption spectra were collected on films deposited on fused silica substrates using a Nicolet Evolution 300 spectrophotometer in the wavelength range 200−800 nm with a scan speed of 500 nm·min^{-1}. Each spectrum is the average of three scans collected with a bandwidth of 1.5 nm, and air was used for the background.

Photoluminescence measurements were performed using a Horiba Jobin Yvon FluoroMax-3 spectrofluorimeter, using a slit aperture of 1 nm with an excitation wavelength of 245 nm (5.06 eV). The probing beam was set to impinge on one side of the sample (silica substrate, incidence angle of 2−3°) so that the sample acted as a waveguide for the incident light wave, while the luminescence was collected at 90° with respect to the incident beam. This configuration enhanced the signal-to-noise ratio and avoided reflection effects. Three acquisitions were averaged for each measurement.

Table 1. Cell Parameters of the Silica−Germania Mesoporous Films Obtained for Different [Ge]/[Si] Molar Ratios, Treated at 100, 350, and 550 °C

sample	cell parameters (nm) at 100 °C	cell parameters (nm) at 350 °C	cell parameters (nm) at 550 °C
SG1	$a = 18$	$a = 15$	$a = 14$
	$c = 16$	$c = 11$	$c = 9$
SG2	$a = 18$	$a = 14$	N/A
	$c = 15$	$c = 10$	N/A

For the UV irradiation experiments, a KFr excimer laser (λ = 248 nm, $E = 5.0$ eV, Lambda Physik, COMPex150, Germany) was used as the excitation source. The irradiation powers and repetition rates were set to ∼220 mJ·cm^{-2} per pulse and 10 Hz.

Results and Discussion

Silica−germania films are generally difficult to prepare via the sol−gel processing due to the different hydrolysis

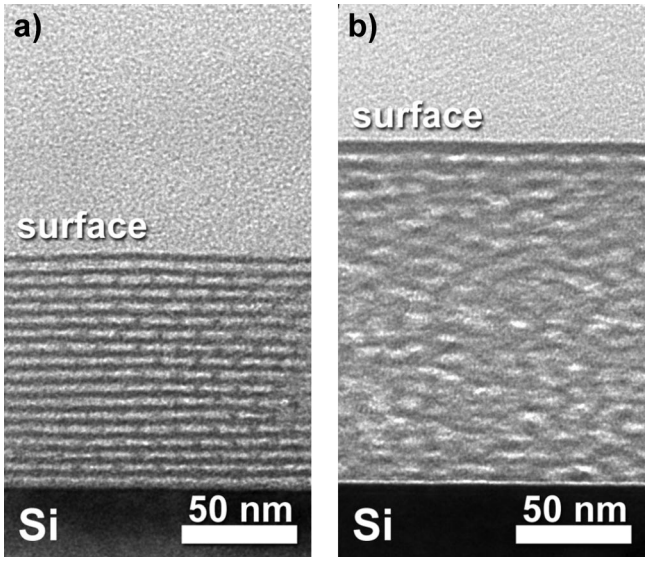

Figure 2. Bright-field cross-section TEM images referring to sample SG1 ([Ge]/[Si] = 0.1), thermally treated at 550 °C (a) and to SG2 ([Ge]/[Si] = 0.2), thermally treated at 350 °C (b).

and condensation rates of the Si and Ge precursors (chlorides or alkoxides).[20] As a consequence, phase separation may occur and homogeneity is difficult to attain;[17b,26] the synthesis is more complex in the case of SiO_2-GeO_2 self-assembled mesostructured films because ordered porosity at the end of the process must be achieved. We have observed that RH is a very critical parameter, and organization is not observed when RH is higher than 25%; after dip-coating the films were colorless and transparent, but if they were not stabilized in the deposition room at low RH for a few minutes after the deposition they quickly turned to white.

The mesostructure of the silica−germania films was analyzed by combining grazing incidence X-ray scattering (GISAXS) with transmission electron microscopy (TEM). The measurements show that the films exhibit a good order with some differences as a function of the composition and temperature. In detail, GISAXS patterns show well-defined spots even for the second order of diffraction, indicating that the mesostructure has a high degree of order upon calcination (Figure 1). The GISAXS patterns were indexed as body-centered tetragonal unit cells belonging to the *I*4/*mmm* symmetry group, in analogy with the structure of hybrid mesoporous films obtained using the same templating agent.[27] The structure is made of ordered mesoporous domains that are randomly oriented around the axis perpendicular to the substrate (*c* axis in the tetragonal system) as it is often the case in mesoporous materials. This is commonly referred to as planar disorder (i.e., the mesostructure has out-of-plane order but lacks in-plane order). The films containing lower Ge content (SG1 and SG2) yielded GISAXS patterns with well defined spots, showing a high degree of order. In the GISAXS patterns of samples with higher Ge content, after thermal treatment at temperatures higher than 100 °C

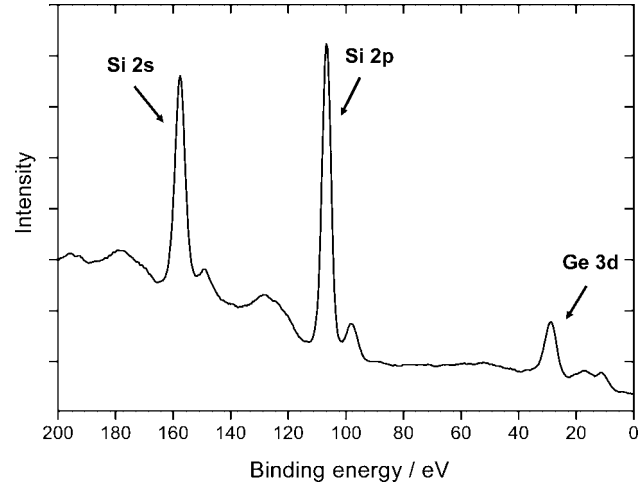

Figure 3. XPS scan of the SG1 sample in the 200−0 eV range.

(SG3 and SG4, not shown in the figure) the spots appear striped along the out-of-plane s_z scattering vector, indicating that the *c* cell parameter (perpendicular to the substrate) is not univocally defined in the region probed by the impinging beam (indicatively, 1 mm^2). In the latter case, therefore, the out-of-plane order of the mesostructure appears to decrease.

The cell parameters were calculated by minimizing an error function defined using the experimental and the theoretical spot positions, as reported elsewhere.[27] In Table 1 the calculated cell parameters for the samples obtained for different Si and Ge compositions, after treatment at 100 and 350 °C, are listed (the full set of GISAXS patterns of the different samples after treatment at 100 °C are reported for comparison in the Supporting Information), as well as the percent contraction of the out-of-plane *c* parameter. Samples SG3 and SG4 gave striped GISAXS patterns when treated at 350 °C; therefore, it was not possible to estimate the cell parameter values, as the error affecting the calculations was too large. Samples SG1 and SG2 treated at 350 °C show a contraction of the *c* parameter, while the *a* and *b* parameters are substantially unaltered within the error bar. GISAXS patterns of films treated at temperatures higher than 350 °C showed a partial or complete loss of order (Figure 1).

Cross-sectional TEM measurements showed a well-ordered mesostructure in sample SG1 thermally treated at 550 °C (Figure 2a). Samples SG2, with respect to SG1, appear less ordered, even for lower temperatures of annealing (350 °C in Figure 2b): in the latter case the regions close to the film−air and film−substrate interfaces appeared more ordered, whereas the central region was found to be highly porous but wormlike. This is an indication that the formation of ordered micellar arrays is nucleated at the interfaces of the film during EISA. Pore morphology is ellipsoidal with the minor axis oriented perpendicular to the substrate; this is because structural shrinkage occurs during drying and calcination. Film thickness was estimated by TEM measurements as (209 ± 3) nm for SG1 samples and (181 ± 3) nm for SG2 samples. The film thickness obtained by spectroscopic ellipsometry is well in accordance with the values of TEM; we calculated (λ = 632.8 nm) 208 (SG1), 206 (SG2), 198 (SG3), and 172 nm (SG4) for the films treated at 350 °C. In the SG1 sample treated at 350 °C, the pore dimensions

(26) Kirkbir, F. Sol-gel process for forming a germania-doped silica glass rod. U.S. Patent 5,254,508, 1993.
(27) Falcaro, P.; Costacurta, S.; Mattei, G.; Amenitsch, H.; Marcelli, A.; Cestelli Guidi, M.; Piccinini, M.; Nucara, A.; Malfatti, L.; Kidchob, T.; Innocenzi, P. *J. Am. Chem. Soc.* **2005**, *127*, 3838.

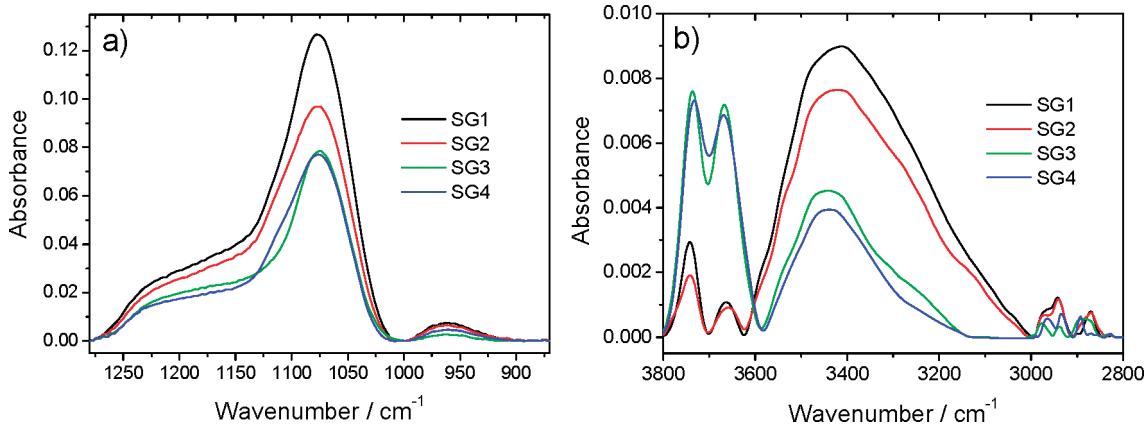

Figure 4. FTIR spectra of the silica−germania films in the 1275−900 cm^{-1} (a) and 3800−2800 cm^{-1} (b) ranges.

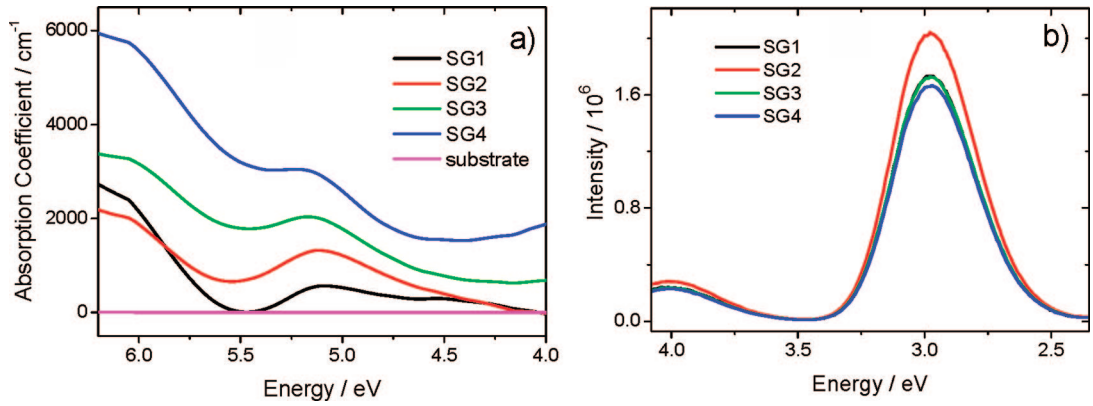

Figure 5. UV−vis absorption (a) and photoluminescence spectra (b) of mesoporous silica−germania films with four different Si and Ge concentrations treated at 350 °C.

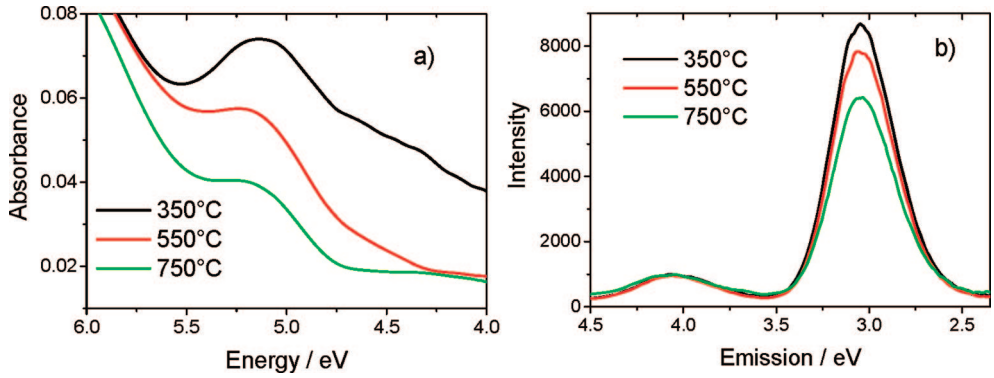

Figure 6. UV−vis absorption (a) and photoluminescence spectra (b) of mesoporous silica−germania SG2 films after thermal treatment at 350, 550, and 750 °C.

measured from the TEM images were 9.0 ($\sigma = \pm$ 1.0 nm) along the major axis a_1, parallel to the surface, and 5.0 nm ($\sigma = \pm$ 1.0 nm) along the minor axis a_2, perpendicular to the substrate. In the SG2 sample treated at 350 °C, the pore dimensions were $a_1 = (2.5 \pm 0.8)$ nm and $a_2 = (2.0 \pm 1)$ nm.

X-ray photoelectron spectroscopy (XPS) was used to investigate the chemical composition of the mesoporous silica−germania films; Figure 3 shows the wide scan XPS spectra of sample SG1. In particular, the Si 2p and Ge 3d XPS spectra were used to estimate the atomic concentration, obtaining an average composition of [Ge]:[Si] = 13:87. The chemical composition was found to be close to the nominal composition, indicating that the final material is not phase-separated; similar results were obtained for the other compositions.

We have also used FTIR analysis to study the structure of the mesoporous silica−germania films at the different compositions. This technique can give information on the presence and nature of surface hydroxyl groups in the material. Figure 4a shows the FTIR absorption spectra in the 1275 −900 cm^{-1} range of the films after treatment at 350 °C. The surfactant is completely removed, as we deduce from the absence of any related absorption mode; the silica antisymmetric stretching mode at 1075 cm^{-1} indicates the formation of a highly interconnected silica backbone;[28] the band at 970 cm^{-1} is attributed to Ge−O−Ge antisymmetric stretching.[29,30] We do not detect the presence the Si−OH

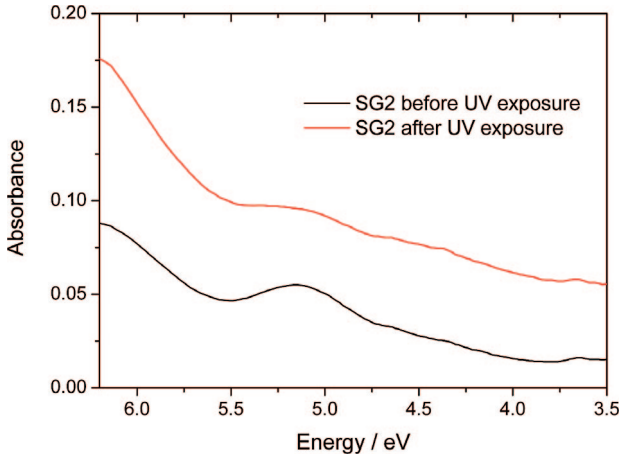

Figure 7. UV−vis absorption spectra of SG2 films before (black line) and after (red line) UV-laser exposure (l = 248 nm).

and Ge−OH bands,[28] which should be present around 930 (Si−-OH stretching) and 750 cm^{-1} (not shown in figure; Ge−OH stretching); this is an indication of the good condensation degree reached by the inorganic silica−germania backbone upon thermal calcination. Figure 4b shows the infrared spectra in the 3800−2800 cm^{-1} interval which is in the range of the stretching modes of O−H groups. The intensity of the bands that are detected is very weak, indicating that most of the hydroxyls were condensed during calcination. The low intensity bands detected in this range give, however, information on the nature of the pore surface after thermal treatment, and in general, single and geminal silanols bands[31] can be observed. The FTIR spectra show three vibrational modes, which change in intensity with the composition: at 3670, 3737, and around 3450 cm^{-1}. The 3670 cm^{-1} band is assigned to OH stretching of SiOH with a contribution from antisymmetric stretching of hydrogen bonded molecular water ($\lambda_{as}(H_2O)$).[32] We attribute the 3737 cm^{-1} band to isolated silanols[33] and the band around 3450 cm^{-1} to OH stretching of silanols that are hydrogen bonded to the oxygen of neighboring silanols ($\lambda_s(OH\cdots{}^{H}OSi)$). The FTIR data suggest that higher concentrations of germania induce a higher silanol condensation because the 3450 cm^{-1} band shifts to higher wavenumbers (which indicates the presence of shorter silanols chains) while the isolated silanols increase in intensity. FTIR spectra give also a good indication of surfactant removal upon thermal treatment at 350 °C, and the C−H stretching bands around 2700 cm^{-1}, which are the typical signature of the surfactant, almost disappeared.

The UV−vis absorption spectra of the films of different compositions, after thermal treatment at 350 °C (Figure 5a), show a band around 5 eV, which is associated with Ge oxygen-deficient centers (GeODC) in the SiO_2−GeO_2 network.[34] These defects consist mainly of twofold coordinated, sp^2-hybridized Ge^{2+} centers with a lone pair of electrons (see ref 35 and references therein). In particular, oxygen-deficient Ge centers (especially divalent Ge^{2+} centers) give rise to photorefractive effects upon irradiation with high-power density UV radiation. Upon UV irradiation, one of these electrons is excited to the conduction band, forming a positively charged Ge center, and then the electron is transferred to an adjacent tetravalent Ge. Two paramagnetic Ge E' centers are eventually formed as a result of electron−hole recombination: this process gives rise to a change in refractive index, due to structural rearrangement and densification of the inorganic network. Therefore, the existence of the 5 eV band suggests the photoactivity of the films. The band around 5 eV can be observed in all mesoporous silica−germania samples obtained with different [Ge]/[Si] ratios, even though it is more intense in the samples with lower Ge content (SG1 and SG2). This result shows that there is not a linear dependence of the absorption coefficient on the Ge concentration in mesoporous silica−germania films. On the basis of the structural characterization of the films we can correlate this property with a lower order of the films at higher Ge content (Figure 1) and a different nature of the pore surface (Figure 4b). The order of the mesophase and the germania content can affect the arrangement of Ge atoms and the ratio between the Ge^{2+} and Ge^{4+} species. This point needs specific further study because the understanding of the defects origin in mesoporous silica−germania films is of paramount interest to develop future applications.

Figure 5b shows the emission photoluminescence (PL) spectrum of the mesoporous silica−germania films with different compositions (λ_{ex} = 245 nm). Intense emission bands at 3.02 eV, together with a less intense peak at 4.07 eV, are observed when the excitation wavelength ranges from 200 to 300 nm. The band at 3.02 eV is attributed to the singlet−triplet emission (β-band) of the Ge^{2+} centers, whereas the band at 4.07 eV is attributed to the singlet−singlet emission of the Ge^{2+} centers (α-band).[36,37]

To elucidate the origin of the absorption band around 5 eV, the SG2 samples were treated at different temperatures. The absorption spectra relative to the SG2 samples show a decrease in intensity of the ∼5 eV band with higher temperatures (Figure 6a). This decrease can be explained by the oxidation of the oxygen-deficient Ge^{2+} centers occurring at higher temperatures: the two-coordinated defects become four-coordinated Ge connected to bridging oxygens. The PL spectra of the SG2 sample treated at different temperatures are shown in Figure 6b. The decrease in intensity of the emitted PL shows that the thermal treatment decreases the concentration of GeODC in the film. This is consistent with an oxidation treatment, which causes the transformation of Ge(II) to Ge(IV).

Preliminary experiments to demonstrate the possibility of producing photoactive silica−germania mesoporous thin

(28) Innocenzi, P. *J. Non-Cryst. Solids* **2003**, *316*, 309.
(29) Jang, J. H.; Koo, J.; Bae, B.-S. *J. Am. Ceram. Soc.* **2000**, *83*, 1356.
(30) Lipinska-Kalita, K. E. *J. Non-Cryst. Solids* **1990**, *119*, 41.
(31) Malfatti, L.; Kidchob, T.; Falcaro, P.; Costacurta, S.; Piccinini, M.; Cestelli Guidi, M.; Marcelli, A.; Corrias, A.; Casula, M. F.; Amenitsch, H.; Innocenzi, P. *Microporous Mesoporous Mater.* **2007**, *103*, 113.
(32) Davis, K. M.; Tomozawa, M. *J. Non-Cryst. Solids* **1996**, *201*, 177.
(33) Innocenzi, P.; Falcaro, P.; Grosso, D.; Babonneau, F. *J. Phys. Chem. B* **2003**, *107*, 711.
(34) Nishii, J. *Mater. Sci. B* **1998**, *54*, 1.
(35) Shigemura, H.; Kawamoto, Y.; Nishii, J.; Takahashi, M. *J. Appl. Phys.* **1999**, *85*, 3413.
(36) Uchino, T.; Takahashi, M.; Yoko, T. *Phys. Rev. Lett.* **2000**, *84*, 1475.
(37) Takahashi, M.; Ichii, K.; Tokuda, Y.; Uchino, T.; Yoko, T.; Nishii, J.; Fujiwara, T. *J. Appl. Phys.* **2002**, *92*, 3442.

films were performed by irradiating the sample SG2 with a KrF excimer laser source at a wavelength of $\lambda = 248$ nm (5.0 eV). Figure 7 shows the absorbance spectra of the films before and after irradiation. The decrease of the 5 eV absorbance peak can be observed; this is accompanied by an increase in the band around 6.3 eV, which is associated with photochemical conversion of divalent Ge defects to Ge E' or Si E'.

Conclusions

We have prepared mesoporous mixed SiO_2-GeO_2 films with variable Si and Ge composition of optical quality. Grazing incidence small-angle X-ray scattering and transmission electron microscopy measurements pointed out that the mesostructure is tetragonal *I*4/*mmm* with a lattice constant on the order of 10 nm. The films with lower Ge have a high degree of order, which is retained even at 550 °C. The silica−germania films after calcinations at 350 °C have a low amount of residual hydroxyls, which appear as isolated silanols and hydrogen bonded short hydroxyl chains. UV−vis absorption and photoluminescence showed that the films possess divalent Ge^{2+} centers.

Acknowledgment. This research was supported by the Italian Ministero dell'Università e della Ricerca (MiUR) through FIRB2003 (RBNE033KMA). Cosmolab Consortium is acknowledged for financial support. We acknowledge the European Synchrotron Radiation Facility (ESRF) for provision of synchrotron radiation facilities and Dr. Peter Boesecke for assistance at beamline ID01. Dr. Junji Nishii, of NIST, Osaka, Japan, is acknowledged for photoactivity experiments.

Supporting Information Available: Additional grazing incidence small-angle X-ray scattering patterns (PDF). This material is available free of charge via the Internet at http://pubs.acs.org.

CM8000249